Correlation between the Knight Shift of Chemisorbed CO and the Fermi Level Local Density of States at Clean Platinum Catalyst Surfaces†

YuYe Tong, Cynthia Rice, Nathalie Godbout, Andrzej Wieckowski,* and Eric Oldfield*

Contribution from the Department of Chemistry, University of Illinois at Urbana-Champaign, 600 South Mathews Avenue, Urbana, Illinois 61801

Received August 24, 1998. Revised Manuscript Received February 18, 1999

Abstract: We have investigated the ^{195}Pt and ^{13}C nuclear magnetic resonance (NMR) spectroscopy of clean-surface platinum catalysts and of CO chemisorbed onto Pt catalyst surfaces. We use Knight shift, relaxation, and *J*-coupling data to deduce information about the Fermi level local density of states (E_f-LDOS) at catalyst surfaces. There is a linear correlation between the Knight shifts of chemisorbed CO and the clean surface E_f-LDOS of platinum onto which the CO is bound, as determined by ^{13}C and ^{195}Pt NMR. The correlation amounts to ∼12 ppm/Ry^{-1}·atom^{-1}, the same as that which can be deduced for CO on palladium, as well as from the electrode potential dependence of ^{13}C Knight shifts and infrared vibrational frequencies, ν_{CO}, and the relationship between ν_{CO} and the E_f-LDOS at clean platinum surfaces. The ability to now directly relate metal and adsorbate electronic properties opens up new avenues for investigating metal−ligand interactions in heterogeneous catalysis and electrocatalysis.

Introduction

Due to its fundamental importance in heterogeneous catalysis, as well as in electrocatalysis, the chemisorption and reaction of CO on transition metal surfaces has been an important focus of modern surface science. Here, the NMR spectroscopy of ^{13}CO adsorbed onto transition metal surfaces has been shown to be a very powerful probe of molecular structure and dynamics of CO itself,[1−8] as well as a probe of the electronic properties of the transition metal surfaces onto which it is adsorbed.[5,7] However, analyses of the relationship between the NMR observables and the electronic properties of a metal's surface are still at an early stage of development. Establishing such a relationship is important, since it should make ^{13}C NMR a powerful and convenient as well as a much more universal microscopic probe, especially in situations where direct NMR studies of the metal are difficult. By combining ^{13}C NMR, ^{195}Pt NMR, and density functional theoretical calculations, we show in this article that there is a linear correlation between the Knight shift of chemisorbed ^{13}CO and the clean surface Fermi level local density of states (E_f-LDOS) of platinum and palladium catalysts. This can be expected to lead to new ways of probing catalyst and electrocatalyst surface structure, including the effects of potential control.

It has long been established, via the unambiguous observation of a Knight shift and the corresponding Korringa relationship, that when ^{13}CO is chemisorbed onto a transition metal surface, either in the gas phase[1] or in an electrolyte solution,[8] that mixing of CO's frontier orbitals, (i.e., 5σ and 2π*) with the transition metal's d band makes the carbon atom become "metallic". It is also generally accepted, at least qualitatively, that the NMR observables of adsorbed ^{13}CO are somehow related to the electronic properties of the metal surface to which it bonds. For example, the dependence of the ^{13}CO line shift on surface composition in a Pt/Rh alloy[6,7] shows that the ^{13}CO shift is a nonlocal property, brought about through alloying. However, no quantitative relationship between ligand shift and the surface E_f-LDOS has yet been reported. Recent theoretical[9,10] and experimental[11,12] studies have tried to quantitatively correlate the spectroscopic properties of adsorbates with the clean surface E_f-LDOS, an attribute of a metal surface *before* chemisorption—a frontier-orbital-interaction approach. For example, it has been shown that a linear correlation exists between the infrared vibrational stretching frequency of chemisorbed CO and the clean surface E_f-LDOS of the metal onto which the CO is adsorbed.[12] This finding suggests that there might be a similar relationship between the Knight shift of chemisorbed ^{13}CO and the clean surface E_f-LDOS. If true, this would represent a significant development in NMR studies of heterogeneous catalysts.

† Supported by the U.S. National Science Foundation (Grant CTS 97-26419), by an equipment grant from the U.S. Defense Advanced Research Projects Agency (Grant DAAH 04-95-1-0581), by the U.S. Department of Energy, Division of Materials Science, through the University of Illinois, Frederick Seitz Materials Research Laboratory (Grant DEFG02-96ER45439), and by use of computational facilities provided by the National Center for Supercomputing Applications (supported by NSF Grant CHE-970020N).

(1) Slichter, C. P. *Annu. Rev. Phys. Chem.* **1986**, *37*, 25−51.
(2) Wang, P.-K.; Ansermet, J.-Ph.; Rudaz, S. L.; Wang, Z. Y.; Shore, S.; Slichter, C. P.; Sinfelt, J. H. *Science* **1986**, *234*, 35−41.
(3) Duncan, T. M. *Colloids Surf.* **1990**, *49*, 11−31.
(4) Duncan, T. M. In *Elementary Reaction Steps in Heterogeneous Catalysis*; Joyner, R. W., van Santen, R. A., Eds.; Kluwer Academic Publishers: Dordrecht, The Netherlands, 1993; pp 221−241.
(5) van der Klink, J. J. *Adv. Catal.* **1999**, *43*, in press.
(6) Ansermet, J.-Ph.; Slichter, C. P.; Sinfelt, J. H. *Prog. NMR Spectrosc.* **1990**, *22*, 401−421.
(7) van der Klink, J. J.; Ansermet, J.-Ph. *J. Catal.* **1997**, *170*, 211−212.
(8) Tong, Y. Y.; Oldfield, E.; Wieckowski, A. *Anal. Chem.* **1998**, *70*, 518A−527A.
(9) Hoffmann, R. *Rev. Mod. Phys.* **1998**, *60*, 601−628.
(10) Feibelman, P. J., Harris, J. *Nature* **1994**, *372*, 135−136.
(11) Tong, Y. Y.; Billy, J.; Renouprez, A. J.; van der Klink, J. J. *J. Am. Chem. Soc.* **1997**, *119*, 3929−3934.
(12) Tong, Y. Y.; Mériaudeau, P.; Renouprez, A. J.; van der Klink, J. J. *J. Phys. Chem.* **1997**, *101*, 10155−10158.

10.1021/ja9830492 CCC: $18.00
Published on Web 03/20/1999

To date, most ^{195}Pt NMR studies have been carried out using oxide-supported catalysts, with the oxide substrates serving to insulate the metal particles from one another. NMR studies of electrocatalysts in an electrochemical environment, i.e., immersed in an electrolyte, are technically more challenging,[8,13−15] since the presence of conducting material in the NMR probe causes extensive magnetoacoustic ringing, rf penetration, and rf noise pickup problems—the latter being more problematic when samples are attached to an external potentiostat. They do, however, offer opportunities to investigate metal−support and metal−ligand interactions which would otherwise be impossible. In addition, they offer the possibility of investigating the effects of electrode potential control.[8,15] Here, we describe the first detailed investigation of the ^{195}Pt NMR line shape, the ^{195}Pt nuclear spin−lattice, and nuclear spin−spin relaxation behavior of such a Pt electrocatalyst. A line shape analysis shows an increase in "healing length" [16] with respect to that observed in the gas phase, that is, the surfaces experience a significant change of their E_f-LDOS in the electrochemical environment. (The "healing length" is a characteristic parameter measuring how fast the platinum atoms recover their bulk properties when moving away from surfaces.) Both Ruderman−Kittel−Kasuya−Yosida[17] (RKKY) *J*-coupling data and Korringa constants,[18] obtained from spin−spin and spin−lattice relaxation rate measurements, respectively, confirm this idea and show a major enhancement in the E_f-LDOS with respect to gas-phase values.[19,20] By combining quantum chemical calculations based on density functional theory (DFT), our current NMR electrochemistry results, and those of "dry" phase surface NMR from the literature, it has been found that, for both Pt and Pd catalysts, the ^{13}C Knight shifts of adsorbed CO are directly proportional to the E_f-LDOS values of clean catalyst surfaces onto which CO is bound, confirming the idea that ligand shifts can be used to probe metal properties.

Experimental Section

Sample Preparation. The electrocatalyst, fuel-cell grade platinum supported on vulcanized (XC-72) conductive graphite, was purchased from E-Tek, Inc. (Natick, MA). The platinum loading and the average particle size, as determined via X-ray diffraction, were the values provided by E-Tek. Preliminary transmission electron microscopy (TEM) results indicate that the particles have a spherical morphology and a narrow particle size distribution. Cleaning of the as-received samples was carried out electrochemically using a three-electrode electrochemical cell, under a continuous stream of ultrapure argon. The supporting electrolyte was 0.5 M H_2SO_4. Once the particles were clean, they were transferred, together with sufficient electrolyte to immerse the electrocatalyst, into an NMR tube, which was then flame-sealed at room temperature, after several pump/purge cycles with ultrapure nitrogen.

NMR Spectroscopy. All measurements were carried out on "home-built" spectrometers equipped with 14.1 and 8.47 T superconducting magnets (Oxford Instruments, Osney Mead, Oxford, U.K.), Tecmag (Houston, TX) Aries data acquisition systems, and an Oxford Instruments CF-1200 cryostat. A Hahn spin−echo pulse sequence ($\pi/2-\tau_0-\pi-\tau_0-$acquire) with 16-step phase cycling, to eliminate ringdown, was used for data acquisition. τ_0 was set to 30 μs. For the ^{195}Pt NMR experiments, which were carried out on the 8.47 T spectrometer, the 90° pulse widths were ca. 5 μs at 80 K and 8 μs at 20 K. A typical repetition rate was about 30 s^{-1}. T_2 was measured by varying τ_0, while T_1 was determined by using a combined saturation-comb spin−echo method. The center frequency was typically between 74 and 78 MHz.

^{13}C NMR measurements were carried out on the 14.1 T spectrometer at room temperature (293 K), at ca. 150.1 MHz. In the presence of conducting materials the *Q*-factor of the probe decreased and the 90° pulse widths increased (from ~8 to 16 μs), so the entire spectral range could not be irradiated uniformly. We therefore used a spin−echo FT mapping technique[21] to more faithfully reproduce the entire spectrum. This technique consists of the following: (a) A series of subechoes were recorded at a constant frequency increment while the carrier frequency was manually switched from one side of the spectrum to the other; (b) After Fourier transformation (FT) of the right-half echo of each subecho, the resulting subspectra were coadded so as to map out the entire spectral region. It has been shown previously[21] that if the frequency increment $\Delta\nu \leq \omega_1(=\gamma H_1)/2\pi$, where H_1 is the radio frequency (rf) field, the mapped spectrum faithfully reproduces the original spectrum. For the experiments here, we used $\Delta\nu = 15$ kHz and seven subspectra were recorded. Composite π pulse $[(\pi/2)_x(4\pi/3)_y(\pi/2)_x]$ excitation was used to invert the ^{13}C spins for inversion−recovery spin−lattice relaxation measurements.

Computational Aspects. Theoretical shielding calculations for $^{13}COPt_7$ and for $^{13}COPd_7$, were performed using the Gaussian-94 suite of programs.[22] We used a G94/DFT calculation to optimize the M−C and C−O bond lengths using a Hay and Wadt/Los Alamos LANL2DZ effective core potential[23] on the metals, a 6-31G* basis on the C,O atoms, and a B3LYP hybrid exchange correlation functional.[24] The M−M internuclear separations were fixed at their bulk values: 2.77 Å (Pt) and 2.75 Å (Pd). The resulting M−C bond lengths were 1.80 Å for both Pt and Pd, with C−O bond lengths of 1.15 Å. We then evaluated the ^{13}C shielding tensors, using a variety of basis sets and functionals, to test the sensitivity of the calculations to these parameters. We first investigated use of B3LYP and BPW91[25] functionals and two basis sets 6-311G(2d) and 6-311++G(2d) on the ligand atoms and LANL2DZ on the metal atoms) for the $COPt_7$ cluster. There was no clear change in shielding when the functionals were varied, so for the $COPd_7$ cluster we used only the B3LYP functional. All calculations were performed on a two four-processor Silicon Graphics/Cray (Mountain View, CA) Origin-200 computers in this laboratory, as well as on SGI/Cray Origin-2000 and Power Challenge systems at the National Center for Supercomputing Applications, located in Urbana, IL.

Theoretical Background for Deducing the Surface E_f-LDOS

For completeness, we provide here a very brief overview of the theoretical background used to determine the platinum

(13) Day, J. B.; Vuissoz, P. A.; Oldfield, E.; Wieckowski, A.; Ansermet, J.-Ph. *J. Am. Chem. Soc.* **1996**, *118*, 13046−13050.
(14) Tong, Y. Y.; Belrose, C.; Wieckowski, A.; Oldfield, E. *J. Am. Chem. Soc.* **1997**, *119*, 11709−11710.
(15) Wu, J. J.; Day, J. B.; Franazczuk, K.; Montez, B.; Oldfield, E.; Wieckowski, A.; Vuissoz, P.-A.; Ansermet, J.-Ph. *J. Chem. Soc., Faraday Trans.* **1997**, *93*, 1017−1026.
(16) Bucher, J.-P.; Buttet, J.; van der Klink, J. J.; Graetzel, M. *Surf. Sci.* **1989**, *214*, 347−357.
(17) Ruderman, M. A.; Kittel, C. *Phys. Rev.* **1954**, *96*, 99−102. Kasuya, T. *Prog. Theor. Phys. (Kyoto)* **1956**, *16*, 45−57. Yosida, K. *Phys. Rev.* **1957**, *106*, 893−898.
(18) Korringa, J. *Physica* **1950**, *XVI*, 601−610.
(19) Rhodes, H. E.; Wang, P.-K.; Stokes, H. T.; Slichter, C. P.; Sinfelt, J. H. *Phys. Rev. B* **1982**, *26*, 3575−3581.
(20) Bucher J. P.; van der Klink, J. J. *Phys. Rev. B* **1988**, *38*, 11038−11047.
(21) Tong, Y. Y. *J. Magn. Res. A* **1996**, *119*, 22−28.
(22) Frisch, M. J.; Trucks, G. W.; Schlegel, H. B.; Gill, P. M. W.; Johnson, B. G.; Robb, M. A.; Cheeseman, J. R.; Keith, T.; Petersson, G. A.; Montgomery, J. A.; Raghavachari, K.; Al-Laham, M. A.; Zakrzewski, V. G.; Oritz, J. V.; Foresman, J. B.; Cioslowski, J.; Stefanov, B. B.; Nanayakkara, A.; Challacombe, M.; Peng, C. Y.; Ayala, P. Y.; Chen, W.; Wong, M. W.; Andres, J. L.; Replogle, E. S.; Gomperts, R.; Martin, R. L.; Fox, D. J.; Binkley, J. S.; Defrees, D. J.; Baker, J.; Stewart, J. P.; Head-Gordon, M.; Gonzalez, C.; Pople, J. A. *Gaussian94*, Revision C.2; Gaussian, Inc.: Pittsburgh, PA, 1995.
(23) Hay, P. J.; Wadt, W. R. *J. Chem. Phys.* **1985**, *82*, 270−283. Wadt, W. R.; Hay, P. J. *J. Chem. Phys.* **1985**, *82*, 284−298. Hay, P. J.; Wadt, W. R. *J. Chem. Phys.* **1985**, *82*, 299−310.
(24) Becke, A. D. *J. Chem. Phys.* **1993**, *98*, 5648−5652. Lee, C.; Yang, W.; Parr, R. G. *Phys. Rev. B* **1988**, *37*, 785−789.
(25) Becke, A. D. *Phys. Rev. A* **1988**, *38*, 3098−3100. Perdew, J. P.; Wang, Y. *Phys. Rev. B* **1992**, *45*, 13244−13249.

surface E_f-LDOS. For more details, the reader is referred to refs 20 and 26−28.

It is well-known that NMR of a metal can be used to deduce a metal's density of states at the Fermi level, since the same Pauli paramagnetism is responsible for both the Knight shift and the nuclear spin−lattice relaxation rate.[29] For transition metals, a phenomenological two-band model was developed some years ago to account for the presence of d-valence electrons.[26] It has been refined more recently[20] and also been put on a solid theoretical basis.[27] Although the d-valence electrons have zero amplitude of their wave function at the nucleus, and therefore do not contribute directly to the Knight shift as do s electrons, they polarize the s-like wave function of the core electrons through exchange interactions, producing the so-called "core polarization" that contributes to the hyperfine contact interaction seen by the nuclei. The model can be mathematically expressed as follows,[11,20,28] for the Knight shift, K, and the spin−lattice relaxation rate, T_1^{-1}:

$$K = K_s + K_d + K_{orb} = \mu_B^2 D_s(E_f) H_{hf,s}/(1 - \alpha_s) + \mu_B^2 D_d(E_f) H_{hf,d}/(1 - \alpha_d) + \chi_{orb} H_{hf,orb}/\mu_B \quad (1)$$

$$S(T_1T)^{-1} = k(\alpha_s)K_s^2 + k(\alpha_d)K_d^2 R_d + [\mu_B D_d(E_f) H_{hf,orb}]^2 R_{orb} \quad (2)$$

where T is the absolute temperature, S is the Korringa constant $(\gamma_s/\gamma_n)^2(h/8\pi^2 k_B)$, μ_B is the Bohr magneton, and χ_{orb} is the orbital susceptibility. $D_s(E_f)$ and $D_d(E_f)$ are the separate s-like and d-like densities of states at the Fermi level. $H_{hf,\lambda}$, with λ = s, d, and orb, stand for s-band, d-band, and orbital contributions; the hyperfine field of the d electrons, $H_{hf,d}$, has a sign opposite to that of $H_{hf,s}$, the hyperfine field of the s-electrons.[26] R_d and R_{orb} are the reduction factors due to the orbital degeneracy at the Fermi level:[26]

$$R_d = [f^2/3 + (1 - f)^2/2] \quad (3)$$

and

$$R_{orb} = 2f(2 - 5f/3)/3 \quad (4)$$

where f is the relative weight of the t_{2g}- and e_g-type d orbitals at the Fermi energy. No interband interactions are taken into account, and the separate s-like and d-like Stoner factors are introduced as

$$\alpha_\lambda = I_\lambda D_\lambda(E_f) \quad \text{with} \quad \lambda = s, d \quad (5)$$

where I_s and I_d are exchange integrals. The relationship between the Stoner and Korringa de-enhancement factors, $k(\alpha)$, are assumed to be given by the Shaw−Warren relationship,[30] for both s-like and d-like electrons alike.

Together with the equation for the total susceptibility, χ, eqs 1 and 2 have been extensively used with bulk platinum NMR by considering I_s, I_d, and $H_{hf,s}$ as fittable parameters, the others being taken from either theoretical calculations or from direct experimental determinations. There has been found to be excellent consistency between experimental and theoretical results. When applied to small platinum particles, only the s- and d-like densities of states were varied, the other parameters being set to those found for bulk Pt.[20] Thus, by evaluating the combined eqs 1 and 2, a pair of experimentally determined K and T_1T can be readily transformed to a pair of s- and d-like E_f-LDOS values, D_s and D_d. Since K can be measured very precisely, the uncertainty in the E_f-LDOS values deduced comes mainly from the uncertainty in T_1T: a 10% uncertainty in T_1T would cause a ~5% uncertainty in the E_f-LDOS values. While there may be even larger systematic errors associated with the simplicity of the model used, the results obtained so far on Pt catalysts after different surface treatments[20,31,32] support the use of the method. And, where E_f-LDOS value have been determined theoretically, they are found to be in good accord with those obtained by NMR.

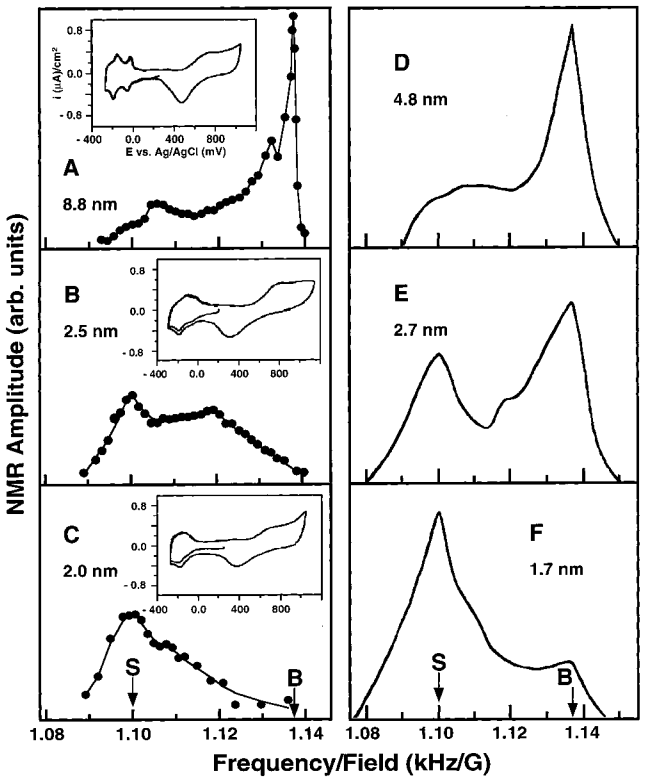

Figure 1. ^{195}Pt NMR spectra (8.47 T), at 80 K, of commercial graphite-supported clean surface nanoscale platinum electrodes with different particle sizes, immersed in 0.5 M H_2SO_4: (A) 8.8 nm; (B) 2.5 nm; (C) 2.0 nm. The insets are cyclic voltammograms for the Pt particles. Reprinted from ref 8. Copyright American Chemical Society 1998. (D−F) ^{195}Pt NMR spectra of Pt on SiO_2 and TiO_2 (gas phase), adapted from ref 34. The "S" and "B" shown on the bottom spectra indicate surface and bulk peak positions, respectively.

Enhancement of the E_f-LDOS at Electrocatalyst Surfaces

By way of introduction to the topic of ^{195}Pt NMR of electrocatalysts, we show in Figure 1A−C the point-by-point particle-size-dependent 8.47 T ^{195}Pt NMR spectra of clean surface nanoscale Pt electrocatalysts in a supporting electrolyte (0.5 M H_2SO_4) recorded at 80 K, obtained in earlier work[8] by

(26) Yafet, Y.; Jaccarino, V. *Phys. Rev.* **1964**, *133*, A1630−A1637. Clogston, A. M.; Jaccarino, V.; Yafet, Y. *Phys. Rev.* **1964**, *134*, A650−A661. Jaccarino, V. *Nuclear Magnetic Resonance and Relaxation in Solids*; van Gerven, L., Ed.; North-Holland Publishing Co.: Amsterdam, 1965; p 23.

(27) van der Klink, J. J. *J. Phys.: Condens. Matter* **1996**, *8*, 1845−1850.

(28) Tong, Y. Y.; van der Klink, J. J. *J. Phys.: Condens. Matter* **1995**, *7*, 2447−2459.

(29) Winter, J. *Magnetic Resonance in Metals*; Clarendon Press: Oxford, U.K., 1971.

(30) Shaw, R. W., Jr.; Warren, W. W., Jr. *Phys. Rev.* **1971**, *B3*, 1562−1568.

(31) Tong, Y. Y.; Martin, G. A.; van der Klink, J. J. *J. Phys.: Condens. Matter* **1994**, *6*, L533 − L538.

(32) Tong, Y. Y.; van der Klink, J. J. *J. Phys. Chem.* **1994**, *98*, 11011−11014.

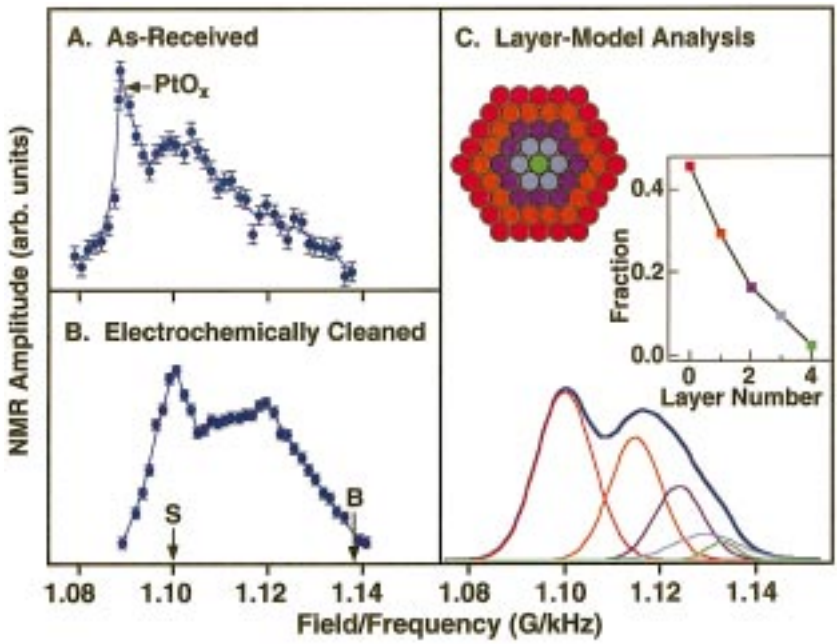

Figure 2. ^{195}Pt NMR spectra showing electrochemical cleaning and a layer-model analysis of the 2.5 nm sample: (A) as received catalyst; (B) electrochemically cleaned in 0.5 M H_2SO_4 (the same spectrum as in Figure 1B); (C) layer-model deconvolution of spectrum B (see text for details). The diagram in part C is a schematic representation of the (111) section of an ideal five-layer cubo-octahedral Pt particle, cutting through the central atom, while the inset in part C shows the layer statistics used for the deconvolution.

manually varying the spectrometer frequency. The insets are the corresponding electrochemical cyclic voltammograms, and the efficiency of the electrochemical cleaning process can be readily appreciated by comparing Figure 2A,B. It has already been demonstrated experimentally, for the case of oxide-supported dry Pt catalysts,[19,20] that the ^{195}Pt NMR spectrum of nanoscale Pt particles is very broad, extending about 4 kG downfield from the position of bulk platinum (1.138 G/kHz) and having a surface peak centered at 1.100 G/kHz. Ab initio relativistic DFT calculations on a five-layer Pt(001) slab have been used to rationalize such a large downfield shift as being due to a gradual drop of d-like E_f-LDOS upon moving from inside the particle to the surface.[33] The size-dependent variations in the electrocatalyst spectra are similar to those observed in conventional dry Pt on oxide supports (Al_2O_3, SiO_2, or TiO_2), as shown in Figure 1E,F[34] and unambiguously demonstrate the presence of a clean surface signal located at ~1.100 G/kHz. This is an interesting observation, given that the electrocatalyst particles not only are supported on a conducting material (graphite) but also are in a supporting electrolyte. However, differences between the wet and dry catalyst spectra can also be seen. In the dry or "gas phase" case, the 2.7 nm sample (Figure 1E) has a larger peak (though broad) at 1.138 G/kHz, the shift position of bulk platinum. Even for the dry 1.7 nm sample (Figure 1F), there is still a bulklike peak at 1.138 G/kHz, although its amplitude is significantly less, and the spectrum is generally quite similar to that we observe for the 2 nm electrocatalyst particles (Figure 1C).

These results indicate that Pt samples prepared by electrochemical cleaning at room temperature are very similar to dry, oxide-supported Pt catalysts of comparable particle size, obtained by high-temperature calcination and reduction, extending several kG downfield from the bulk position. From the particle size dependence, we conclude that the clean surface signal in the electrocatalyst is centered at about 1.100 G/kHz, as found in the gas-phase case.[20] However, the high-field side of the clean surface spectrum is noticeably compressed toward the low-field side, suggesting an increase in the healing length of the particles. If the size distribution of a sample is known, it is possible to use a simple layer model to deconvolute the spectrum and deduce the healing length, since a particle can be viewed as being built up, layer-by-layer, from a central atom.[16] The "layer model" assumes that the NMR signal within a given layer, n, can be represented by a Gaussian. When moving from the surface toward the inside of a particle, the center of the Gaussian (that is, the Knight shift of that layer) "heals" back exponentially toward the bulk platinum position, as follows:[16]

$$K_n = K_\infty - (K_0 - K_\infty)\exp(-n/m) \qquad (6)$$

Here, n is the layer number, counting inward from the surface layer (where $n = 0$), m is the characteristic number (of layers) defining the "healing length" for the Knight shift, and K_0 and K_∞ are the Knight shifts of the surface layer and the bulk, respectively. Applying this analysis to the 2.5 nm sample and assuming ideal cubooctahedral morphology (see diagram in Figure 2C) and a uniform particle diameter of $d = 2.5$ nm (based on X-ray diffraction data), we obtain the layer statistics shown in the inset of Figure 2C. This results in the ^{195}Pt NMR spectral deconvolution shown in Figure 2C, which is in good accord with the experimental result, shown in Figure 2B. The healing length, defined as m times the distance between two consecutive layers (0.229 nm for Pt), is, however, 0.46 nm ($m = 2$ Pt layers) from the deconvolution, which is to be compared with 0.31 nm ($m = 1.35$ Pt layers) in the gas-phase case (16), indicating a significant change in the electronic structure of the carbon-supported sample.

More detailed information about the changes in surface electronic properties, i.e., an increase or a decrease in the clean surface E_f-LDOS, can be obtained from an analysis of the spin−lattice (T_1) and spin−spin (T_2) relaxation data. Typical results are shown in Figure 3. These relaxation curves were measured at 1.100 G/kHz (surface) and 1.1195 G/kHz (about 2.5 layers

(33) Weinert, M.; Freeman, A. J. *Phys. Rev. B* **1983**, *28*, 6262−6269.
(34) Bucher, J. P. Ph.D. Thesis, École Polytechnique Fédérale de Lausanne, Switzerland, 1988.

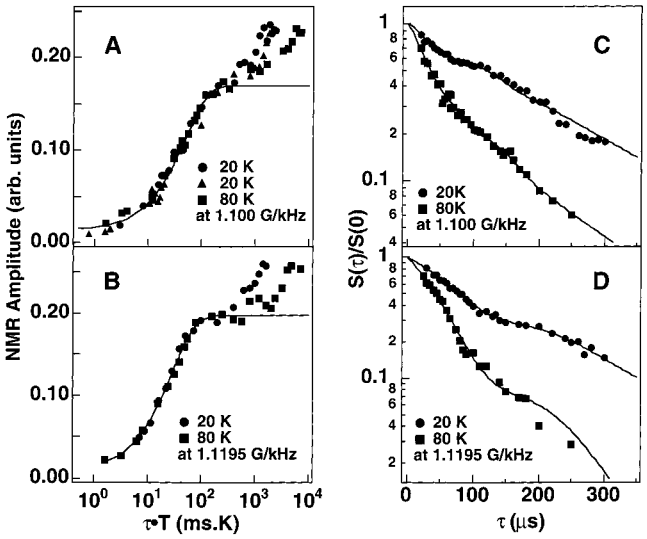

Figure 3. ^{195}Pt spin−lattice and spin−spin relaxation data for Pt electrocatalyst samples: (A and B) spin−lattice (T_1) relaxation curves, taken at 20 and 80 K; (A) data points measured at 1.100 G/kHz (circles and triangles were data from two independent measurements at 20 K); (B) at 1.1195 G/kHz [The time axes were scaled by the temperature at which the measurements were performed, and the amplitudes were normalized, as discussed in the text. The solid lines are single exponential fits for the rapidly relaxing component, at both 20 and 80 K]; (C and D) spin−spin (T_2) relaxation data taken at 20 K and at 80 K; (C) data points measured at 1.100 G/kHz; (D) at 1.1195 G/kHz. The solid lines are the fits to eq 7.

deep inside the particles, Figure 2C), at 80 and 20 K (two samples), for $d = 2.5$ nm samples. At both 1.100 and 1.1195 G/kHz, the T_1 curves (Figure 3A,B) show two well-separated relaxation components. This is most readily seen in data which have been temperature-scaled and amplitude-normalized. The amplitude normalization factor was determined from a single exponential fit of the fast relaxation component. The temperature scaling factor follows Curie law behavior, within experimental error. As noted previously,[32,35] a Korringa mechanism[18] requires that if there is no temperature-dependent change in the E_f-LDOS, then such spin−lattice relaxation results will fall onto a single curve, even though the curve is nonexponential. This is indeed the case for the rapidly relaxing components, both at 1.100 and at 1.1195 G/kHz, showing that both these components follow the Korringa relationship, a fingerprint of the metallic state.

Now, it is not uncommon in the case of oxide-supported small platinum particles to find that the spin−lattice relaxation behavior of the surface platinum atoms is nonexponential. For example, when all surface atoms are in the metallic state, the whole relaxation curve measured at different temperatures can be scaled into one single curve.[32,35] However, this is not the case for the slowly relaxing component in the carbon-supported electrocatalyst samples shown in Figure 3A,B (the clusters of points to the top right). Even more surprising is the observation that the slowly relaxing component has a smaller T_1T at low temperatures than at high temperatures, suggesting a more efficient relaxation mechanism at low temperature. A likely explanation for these results is that the slower relaxing component arises from a strong interaction between the platinum atoms and the carbon support, which produces a sharp feature in the LDOS around the Fermi level, for those platinum atoms.

To test this idea, we chemisorbed CO (via methanol electrodecomposition[13] to a surface coverage of 0.56 monolayer

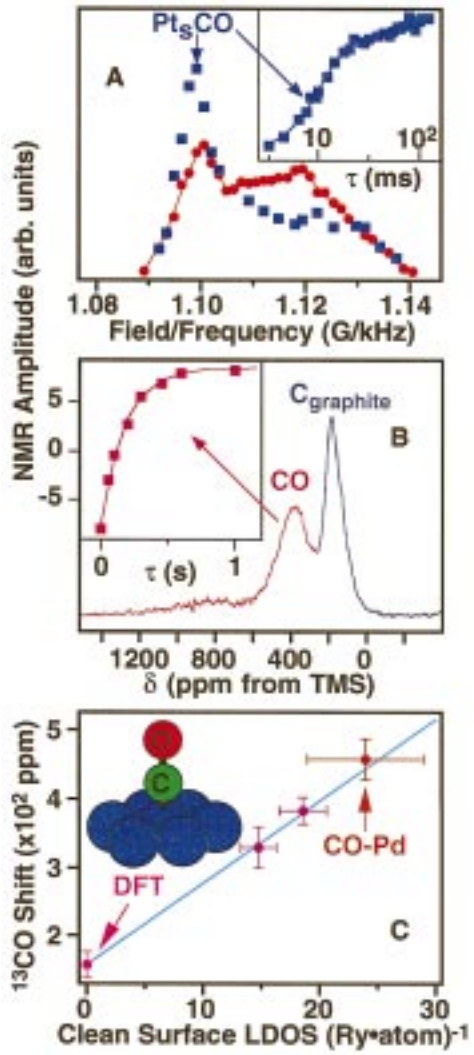

Figure 4. ^{195}Pt and ^{13}C NMR results for CO on Pt: (A) Point-by-point ^{195}Pt NMR spectra of clean Pt particles (red circles) and Pt particles with adsorbed CO (blue squares). Inset shows a typical spin−lattice relaxation recovery curve measured at 1.099 G/kHz (the maximum peak intensity in the spectrum) and at 80 K for ^{195}Pt having adsorbed CO (2.5 nm particles). The ^{195}Pt T_1 values are 1.15 and 37.2 ms, for fast and slow components, respectively. (B) Typical ^{13}C NMR spectrum for ^{13}CO on Pt together with associated spin−lattice relaxation behavior (inset). (C) Correlation between the Fermi level total electronic densities of states for Pt (in Ry^{-1}•atom^{-1}) and the ^{13}CO Knight shift. The inset structure shows the $COPt_7$ cluster used to evaluate the purely orbital contribution to shielding and is basically the same as that used for evaluating the orbital contribution for ^{13}CO on Pd metal (top right point). Also shown in the single data point for CO on Pd not included in the correlation (see text for details). The slope and R^2 values for the three Pt points are 11.9 ± 0.4 ppm/Ry^{-1}•atom^{-1} and 0.999, or with the Pd datum, slope = 12.3 ± 0.4 ppm/Ry^{-1}•atom^{-1} and $R^2 = 0.999$. For comparison, the empirical result based on the potential dependence of IR and NMR peak shifts was slope = 9.5 ppm/Ry^{-1}•atom^{-1}.

(ML)) onto the electrode surfaces and measured the ^{195}Pt spin−lattice relaxation at the surface spectral position, as shown in Figure 4A. These results indicate that chemisorption of CO doubles the relaxation time of the fast component, but not the slow one. The two-exponential fit shown in the inset of Figure 4A gives the same relaxation time for the slow component (Table 2) with or without surface CO adsorption. This means that the slow component arises from platinum atoms which are not accessible to the adsorbate, possibly platinum atoms having a strong interaction with the supporting carbon substrate. The

(35) Tong, Y. Y.; Laub, D.; Schulz-Ekloff, G.; Renouprez, A. J.; van der Klink, J. J. *Phys. Rev. B* **1995**, *52*, 8407−8413.

Table 1. ^{195}Pt NMR Data at Solid/Liquid and Solid/Gas Interfaces

	solid/liquid	solid/gas
healing length (nm)	0.46	0.31[a]
J (kHz)	7.9	4.2[b]
D_s (Ry^{-1}·atom^{-1})	5.1 (5.6)	3.9[c] (4.1)
D_d (Ry^{-1}·atom^{-1})	13.5	10.9[c]
D_{total} (Ry^{-1}·atom^{-1})	18.6	14.8[c]

[a] Reference 16. [b] Reference 19. [c] Reference 20. The numbers in parentheses were calculated from eq 9.

Table 2. Spin−Lattice Relaxation Results for ^{195}Pt[a]

sample	clean surfaces	PtCO
A_1	0.68 ± 0.01	0.80 ± 0.02
$T_{1,\,fast}$ (ms)	0.62 ± 0.03	1.15 ± 0.09
$T_{1,\,slow}$ (ms)	37.3 ± 6.8	37.2 ± 11.9

[a] The results are for the best fit to a five-parameter double-exponential function $\{A_0 + [A_\infty - A_0][1 - A_1 \exp(-t/T_{1,fast}) - (1 - A_1) \exp(-t/T_{1,slow})]\}$ for the nuclear spin−lattice relaxation data measured at the surface peak position and at 80 K for clean and CO chemisorbed surfaces. A_0 and A_∞ are the residual and fully relaxed signal amplitudes, A_1 the amplitude fraction of fast relaxing component with relaxation time $T_{1,fast}$, and $T_{1,slow}$ is the relaxation time for the slow component.

increase in fraction A_1 for PtCO is consistent with the narrowing of the surface peak upon chemisorption. The slow component at 1.1195 G/kHz also appears to have the same origin as that at 1.100 G/kHz, based on their virtually identical temperature dependences (Figure 3A,B). Since the slow component appears to relate to platinum atoms which are not accessible to the adsorbate, we shall not analyze them further. They do, however, suggest the presence of a strong metal−support interaction.

We now analyze the ^{195}Pt relaxation results in more detail. The solid lines in Figure 3A,B are from a single-exponential fit of the fast relaxation component taken at both 20 and 80 K and yield $T_1T = 49.1 \pm 2.6$ ms·K at 1.100 G/kHz and 29.5 ± 1.5 ms·K at 1.1195 G/kHz. This rapidly relaxing component comprises 70 and 76% of the total at the two respective positions. Without resorting to any detailed theoretical model, just by comparing T_1T with the value measured at 1.100 G/kHz for a clean surface oxide-supported platinum catalyst,[20] we can immediately state that there is in fact a major enhancement in the clean surface E_f-LDOS at the electrocatalyst surface, since $T_1T = 103 \pm 7$ ms·K for the gas-phase system.[20] By knowing the Knight shift (the spectral position) and the corresponding T_1T values, we can next deduce the s- and d-like E_f-LDOS, D_s and D_d, from eqs 1 and 2. For the clean electrocatalyst surface we find $D_s = 5.1 \pm 0.3$ Ry^{-1}·atom^{-1} and $D_d = 13.5 \pm 0.6$ Ry^{-1}·atom^{-1}, for a total E_f-LDOS of 18.6 Ry^{-1}·atom^{-1}. The corresponding gas-phase values are 3.9 ± 0.6 and 10.9 ± 0.5 Ry^{-1}·atom^{-1},[20] for a total E_f-LDOS of 14.8 Ry^{-1}·atom^{-1}. This represents a 26% enhancement in the total E_f-LDOS at the clean electrocatalyst surface, immersed in an electrolyte, with respect to that at a clean oxide-supported dry catalyst surface (i.e., under vacuum).

Next, we investigate the T_2 results shown in Figure 3C,D, to obtain complementary information on the E_f-LDOS to that obtained from T_1, and the spectral line shape. The echo decays can be fit to the following equation:

$$S(t)/S_0 = A_0 \exp(-2t/T_2^{f})\{B_0 + \exp(-(t/T_{2j})^2)[B_1 \cos Jt + B_2 \cos 2Jt]\} + A_1 \exp(-2t/T_2^{s}) \quad (7)$$

where A_0 and A_1 are, respectively, the fractions of the fast and the slow relaxing components, J is the RKKY J-coupling constant, and the other terms are as described by Slichter and co-workers.[19] The best fits gave the results collected in Table 3, which also includes the T_1T results. As expected, we find an A_0 value of ∼0.76, *the same as deduced from the T_1 measurements*, but the J-couplings vary, depending on where they are measured. The increase in B_0 at 20 K was due to the longer $\pi/2$ pulse used to prevent arcing problems. At the 1.100 G/kHz surface peak position, J varies from 7.9 ± 0.6 kHz at 20 K to 6.6 ± 1.1 kHz at 80 K, while at a position 2.5 layers below the surface, $J = 3.8 \pm 0.3$ kHz at 20 K and 3.9 ± 0.4 kHz at 80 K, bulk values. To date, there are no published J values available at the solid−gas interface (i.e., at ∼1.100 G/kHz) which might permit a direct comparison with the results obtained in the electrochemical environment, but as expected, the value of 4.2 kHz found at 1.117 G/kHz is the same as that found previously for bulk platinum.[19] In addition, another result, found for a dry 2.1 nm poly-*N*-vinyl-2-pyrrolidone protected platinum sample, at 1.100 G/kHz (the clean surface peak position) is $J = 3.2$ kHz.[14,36] If the influence of PVP is minor, as suggested previously,[37] then 3.2−4.2 kHz is a reasonable estimate of J at a clean solid−gas interface. This is also consistent with the observation that the dry, clean surface s-like E_f-LDOS (3.9 Ry^{-1}·atom^{-1} [20]) is very close to that of the bulk (4.08 Ry^{-1}·atom^{-1} [38]).

Table 3. Spin−Lattice and Spin−Spin (J-Coupling) Results for ^{195}Pt Catalysts[a]

	1.100 G/kHz		1.1195 G/kHz	
	20 K	80 K	20 K	80 K
T_1T (ms·K)	49.1 ± 2.6		29.5 ± 1.5	
$J/2\pi$ (kHz)	7.9 ± 0.6	6.6 ± 1.1	3.8 ± 0.3	3.9 ± 0.4
T_2^f (μs)	373 ± 18	103 ± 52	342 ± 15	160 ± 20
T_{2j} (μs)	144 ± 75	822 ± 789	265 ± 80	321 ± 150
T_2^s (μs)	379 ± 30	312 ± 200	305 ± 50	143 ± 60
B_0	0.88 ± 0.03	0.76 ± 0.12	0.80 ± 0.03	0.69 ± 0.05
B_1	0.10 ± 0.03	0.19 ± 0.09	0.20 ± 0.03	0.31 ± 0.05
A_0	0.77 ± 0.06	0.71 ± 0.06	0.80 ± 0.06	0.88 ± 0.14

[a] The results shown represent the best fits to a single exponential for T_1 for the data shown in Figure 3A,B. The T_2/J-coupling data were obtained by using eq 7 to fit the results shown in Figure 3C,D, as discussed in the text.

Quite clearly then, these results show that the RKKY J-couplings of platinum atoms at the solid−liquid interface are enhanced by about a factor of 2 with respect to those at the solid−gas interface, a view which is completely consistent with the T_1T and line shape results described above.

Since it is believed that the RKKY J-coupling constant is mainly determined by the s-like E_f-LDOS,[37,39] we can write down, by assuming $J/J_{bulk} = K_s/K_{s,bulk}$ (where K_s is the Knight shift of the s-like electrons) and by taking into account the effect of Stoner enhancement,[30] the following equation for the s-like E_f-LDOS of platinum:

$$D_s(J) = [I_s + (J_{bulk}/J)(1 - I_s D_{s,bulk})/D_{s,bulk}]^{-1} \quad (8)$$

where I_s is the exchange integral for s-like electrons. By taking $J_{bulk} = 4.2$ kHz,[19] $D_{s,bulk} = 4.08$ Ry^{-1}·atom^{-1},[38] and $I_s = 0.098$ Ry,[20] eq 8 becomes

$$D_s(J) = (0.098 + 0.63/J)^{-1} \quad (9)$$

For $J = 7.9$ kHz, $D_s(J) = 5.6$ Ry^{-1}·atom^{-1}. This is quite close

(36) Tong, Y. Y.; van der Klink, J. J. Unpublished work.
(37) Tong, Y. Y.; Yonezawa, T.; Toshima, N.; van der Klink, J. J. *J. Phys. Chem.*, **1996**, *100*, 730−733.
(38) MacDonald, A. H.; Daams, J. M.; Vosko, S. H.; Koelling, D. D. *Phys. Rev. B* **1981**, *23*, 6377−6398.
(39) Narath, A.; Weaver, H. T. *Solid State Commun.* **1968**, *6*, 413−415.

to the $D_s = 5.1 \pm 0.3$ $Ry^{-1}\cdot atom^{-1}$ value found from the ^{195}Pt NMR T_1 measurements described above.

At the bulk resonance position for the electrocatalyst (1.1195 G/kHz), $T_1T = 29.5$ ms·K and $J = 4$ kHz, the same values as those found for bulk platinum metal. Indeed, the total E_f-LDOS in the electrocatalyst sample (as deduced from the two-band model calculation[20]) is 24.1 $Ry^{-1}\cdot atom^{-1}$, with $D_s = 5.3$ $Ry^{-1}\cdot atom^{-1}$ and $D_d = 18.8$ $Ry^{-1}\cdot atom^{-1}$. This indicates that, at this internal position (about 2.5 atomic layers deep from the surface, see Figure 2C), the platinum atoms have almost "healed" back to their bulk property values.

As may be seen from Table 1, surface platinum atoms in the carbon-supported electrocatalyst samples, in an electrolyte solution, experience major electronic changes with respect to those in solid/gas systems. In particular, there is significant enhancement in the E_f-LDOS in the electrocatalyst samples. While we cannot say that these effects are solely due to the presence of the electrochemical interface, the alternative possibility that these effects are solely due to the support seems implausible, since the surface atoms are typically some tens of angstroms separated from the metal−support interface, while the electrolyte molecules are directly situated at the surface. Most likely, both effects are operative, although for our present purpose—the investigation of correlations between metal catalyst properties (E_f-LDOS) and adsorbate properties (the ^{13}C Knight shift), the exact breakdown is unimportant.

Correlation between the Clean-Surface E_f-LDOS at the Surfaces of Platinum Catalysts and the ^{13}C Knight Shift of Chemisorbed CO

We now consider the ^{13}C NMR results and their possible relationship to the metal NMR data. We show in Figure 4B the spin−echo FT mapping[21] ^{13}C NMR spectrum of CO adsorbed onto the surfaces of a 2.5 nm sample, prepared via the electrodecomposition of methanol.[13] While the peak at ca. 170 ppm in the ^{13}C NMR spectrum coincides with that of graphite,[40] the peak at ∼383 ppm arises from ^{13}CO bonded to surface Pt atoms, and has a T_1 value at 293 K of 180 ms (inset of Figure 4B). The large frequency shift is the result of a combined Knight shift plus the ubiquitous orbital or chemical shift. At lower coverage (<0.3 vs 0.56 ML) a second species has been identified[40] and attributed to bridge-bound CO, but at high coverage, most CO is expected to be linearly bound to platinum.

Technically, it is of course difficult to separate the Knight shift from the purely orbital or chemical shift of the chemisorbed CO. The traditional approach has been to use transition metal carbonyl clusters as references for the orbital or chemical shift contribution.[1] However, since the bonding in metal carbonyls may be somewhat different to that in systems containing large numbers of metal atoms, equating the orbital (chemical) shift of a metallic carbonyl to that of a molecular carbonyl is worth further investigation. We therefore used density functional theory (DFT) calculations to deduce the chemical shift of CO on model metal atom surfaces. The models used are an on-top $COPt_7$ and $COPd_7$ clusters, shown schematically in the inset in Figure 4C. Such small clusters are not highly metallic and should therefore give a good zero point reference for the purely orbital or chemical shift. We found, for the purely orbital or chemical shift for $COPt_7$, a value of 160 ± 20 ppm from tetramethylsilane (TMS). The standard deviation accounts for the variation due to use of different functionals and basis sets. This is in very good agreement with a value of 167 ppm, reported for $[Pt_{19}(CO)_{12}(\mu_2\text{-}CO)_{10}]^{4-}$.[41] For $COPd_7$, we found an isotropic shift of 203 ± 20 ppm, which is also in good agreement with available experimental data.[42,43] It is of some interest that within the uncertainty of the DFT calculations, the chemical shifts of on-top $COPt_7$ and $COPd_7$ clusters are in excellent agreement with those of the metal carbonyls measured experimentally. Such a theoretical approach may be applicable to other metals as well, including systems where cluster compound results are not available.

Table 4. Correlation between Clean Surface E_f-LDOS and ^{13}C Shift of Chemisorbed CO (Knight Shift = Total Shift − Chemical Shift)

sample	clean surface E_f-LDOS ($Ry^{-1}\cdot atom^{-1}$)	total ^{13}C shift of $CO_{chemisorbed}$ (ppm w.r.t TMS)
$PtCO_7$	0	160 ± 20[a]
CO−Pt/oxides (dry)	14.8 ± 1.5[b]	330 ± 30[c]
CO−Pt/carbon (wet)	18.6 ± 2.0[d]	383 ± 20[d]
$PdCO_7$	0	203 ± 20[a]
CO−Pd/oxides (dry)	24 ± 5[e]	500 ± 30[f]

[a] Evaluated by using density functional theory. The total shift here is just the chemical or orbital shift. [b] From ref 20. [c] From refs 1 and 44. [d] This work. [e] From refs 38 and 47. [f] From ref 46.

Finally, we consider the relationship between the Knight shift of chemisorbed ^{13}CO and the corresponding clean surface E_f-LDOS of the metal onto which the CO is chemisorbed, both for Pt and Pd. In the gas-phase case, Bucher and van der Klink found 14.8 $Ry^{-1}\cdot atom^{-1}$ for the clean surface E_f-LDOS of Pt/TiO_2[20] and Slichter and co-workers found a frequency shift of 330 ppm for ^{13}CO adsorbed on Pt/η-Al_2O_3, which was coverage independent.[1,44] Since it has also been shown previously[45] for clean-surface Pt−oxide catalysts that the spin−lattice relaxation rate, i.e., the surface E_f-LDOS, is independent of the choice of support material (silica, alumina, or titania) and of the method of preparation (ion exchange, colloidal process, or impregnation), it is reasonable to correlate the ∼330 ppm frequency shift of adsorbed CO with a value of 14.8 $Ry^{-1}\cdot atom^{-1}$ for the clean surface E_f-LDOS, in the gas-phase system.

We therefore have for the Pt−CO system: an orbital shift of 160 ppm from theory and organometallic model systems, corresponding to an E_f-LDOS = 0; the 330 ± 30 ppm orbital-plus-Knight shift of CO on Pt/oxide supports having E_f-LDOS = 14.8 $Ry^{-1}\cdot atom^{-1}$; and the 383 ppm, 18.6 $Ry^{-1}\cdot atom^{-1}$ value for the electrocatalyst. These results are shown numerically in Table 4 and graphically in Figure 4C. The line is the linear fit to the three points for Pt and has an R^2 value of 0.999, a slope of 11.9 ± 0.4 ppm/$Ry^{-1}\cdot atom^{-1}$, and an intercept of 158 ± 6 ppm.

This is an interesting result since it supports the hypothesis that the ^{13}CO Knight shift is directly related to the clean surface Fermi level local density of states, but obviously this is also a very limited data set. Fortunately, there are two other *independent* pieces of information which we can relate to the results shown in Figure 4C. The first involves the ^{13}CO−Pd system. Here, for on-top adsorption of CO on Pd, the ^{13}C shift is 500 ± 30 ppm.[46] There is no direct measurement of the clean surface E_f-LDOS for Pd available, but an estimate has been made[47]

(40) Yahnke, M. S., Rush, B. M., Reimer, J. A., Cairns, E. J. *J. Am. Chem. Soc.* **1996**, *118*, 12250−12251.

(41) Washecheck, D, M.; Wucherer, E. J.; Dahl, L. F.; Geriotti, A.; Longini, G. *J. Am. Chem. Soc.* **1979**, *101*, 6110−6112.

(42) Bradley, J. S.; Millar, J.; Hill, E. W.; Melchior, M. *J. Chem. Soc., Chem. Commun.* **1990**, 705−706.

(43) Zilm, K, W.; Bonneviot, L.; Haller, G. L.; Han, O. H.; Kermarec, M. *J. Phys. Chem.* **1990**, *94*, 8495−8498.

(44) Dean, E. J. Ph.D. Thesis, University of Illinois at Urbana-Champaign, 1997.

(45) van der Klink, J. J. *Z. Phys. D* **1989**, *12*, 327−330.

based on the changes in magnetic susceptibility of small Pd particles with respect to their bulk value, by application of the exponential healing model.[16] While keeping the s-LDOS constant, it was found that the d-LDOS at the surface equals two-thirds that of the bulk. For bulk Pd, one has s-LDOS = 3.34 $Ry^{-1}\cdot atom^{-1}$ and d-LDOS = 30.6 $Ry^{-1}\cdot atom^{-1}$.[38] We therefore obtain for the clean Pd surface, E_f-LDOS = 24 $Ry^{-1}\cdot atom^{-1}$. The theoretical calculation of the ^{13}C shift for $COPd_7$ gives δ_{iso}= 203 ppm. After correcting for this chemical or orbital shift for CO−Pd, the purely Knight shift for ^{13}CO on Pd falls very close to the straight line relation, as shown in Figure 4C. Indeed, the slope calculated from the two points available for the Pd−CO system is 12.4 ppm/$Ry^{-1}\cdot atom^{-1}$.

The second confirmation comes from a simple analysis of previously published NMR and infrared data, as has been briefly discussed by us previously.[8] In particular, it has been found that, for CO on Pt surfaces, there exists a linear relationship between the infrared vibrational stretching frequency,[48] as well as the ^{13}C shift,[15,49] and the externally applied electrical potential in an electrochemical cell. This yields a linear IR− ^{13}C NMR correlation. It has also been shown that there exists a linear relationship between the IR vibrational stretching frequency and the clean surface E_f-LDOS in the gas phase.[12] When combined, these results lead to a linear ^{13}C shift/E_f-LDOS correlation. The slopes are respectively 30 cm^{-1}/V, − 71 ppm/V, and −4 cm^{-1}/$Ry^{-1}\cdot atom^{-1}$, from which one then readily deduces a slope of 9.5 ppm/ $Ry^{-1}\cdot atom^{-1}$.[8] This is in very good agreement with the slope of 11.9 ppm/$Ry^{-1}\cdot atom^{-1}$ found in Figure 4C. The great similarity between these two sets of experiments strongly indicates that the potential dependence of the ^{13}C shift, as well as the IR vibrational stretching frequency of adsorbed CO, is dominated by changes in the E_f-LDOS.

Conclusions

The linear relationship found in Figure 4C is, we believe, a rather interesting result. In particular, it suggests a perhaps universal relationship (at least for on-top chemisorption) between the ^{13}C Knight shift of chemisorbed CO and the clean surface E_f-LDOS of the transition metal onto which the CO is adsorbed:

$$\delta(^{13}C) = a\cdot \mathrm{LDOS(Pt)}$$

where $a \sim 11\ (\pm 2)$ ppm/$Ry^{-1}\cdot atom^{-1}$. This finding is in full agreement with the frontier-orbital-interaction picture of metal surface chemistry,[9,10] in which the importance of the clean surface E_f-LDOS is emphasized, and also puts for the first time the NMR spectroscopy of chemisorbed CO on a more quantitative basis for probing the electronic properties of transition metal surfaces.

Acknowledgment. Y.Y.T. thanks Dr. J. J. van der Klink (EPFL, Switzerland) for useful discussions.

JA9830492

(46) Becerra, L. R.; Slichter, C. P.; Sinfelt, J. H. *Phys. Rev. B* **1995**, *52*, 11457−11462.

(47) van der Klink, J. J. In *Physics and Chemistry of Ginite Systems: From Cluster to Crystals*; Jena, P., et al., Eds.; Kluwer Academic Publishers: Dordrecht, The Netherlands, 1992; Vol. I, pp 537−547.

(48) Kunimatsu, K.; Seki, H.; Golden, W. G.; Gorden, J. P.; Philpott, M. R. *Surf. Sci.* **1985**, *158*, 596−605. Zou, S.; Weaver, M. J. *J. Phys. Chem.* **1996**, *100*, 4237−4242.

(49) Vuissoz, P.-A.; Ansermet, J.-Ph.; Wieckowski, A. *Electrochim. Acta* **1998**, *44*, 1397−1401.